

Influence of Fe-Site Substitutions upon Intragrain and Intergrain Magnetoresistance in the Double-Perovskite $\text{Ba}_2\text{FeMoO}_6$

F. Sriti, A. Maignan, C. Martin,* and B. Raveau

Laboratoire CRISMAT, UMR 6508 associée au CNRS, ISMRA et Université de Caen 6, Boulevard du Maréchal Juin, 14050 Caen Cedex, France

Received November 27, 2000. Revised Manuscript Received February 23, 2001

Transport and magnetic properties are significantly influenced by the substitution of various divalent (Mg, Zn, Ca) and trivalent (Cr, Mn, In, Y) cations for iron in the double-perovskite $\text{Ba}_2\text{FeMoO}_6$. An increase of the resistivity and a spectacular decrease of ferromagnetism, especially of T_C , are observed as the substitution level increases. Both intragrain magnetoresistance (MR), characterized by a peak of the resistance ratio around T_C , and intergrain tunnel magnetoresistance (TMR), at low temperature, are observed. The substitution does not kill the TMR because the TMR effect is obtained for the substitution level as high as 40% on the Fe site. More importantly, high TMR magnitudes are observed for zinc-substituted oxides.

Introduction

The discovery of tunneling magnetoresistance (TMR) at room temperature and at low magnetic field in the ordered ferrimagnetic metallic double-perovskite $\text{Sr}_2\text{FeMoO}_6$ ¹ has shown the great potentiality of this oxide for magnetic recording compared to manganites for which the appearance of intergrain TMR is much smaller and requires to work below room temperature.² The evidence for intergrain TMR in polycrystalline $\text{Sr}_2\text{FeReO}_6$ ³ and in $\text{Ba}_2\text{FeMoO}_6$ ⁴ shows that the double perovskites that have semimetallic properties and exhibit ferromagnetism should be considered as competitive materials for magnetoresistance applications. It was previously demonstrated^{1,5–8} that TMR is strongly dependent on the carrier scattering at the grain boundary of the polycrystalline oxide and consequently is very sensitive to the magnetic field. Nevertheless, the investigation of $\text{Ba}_2\text{FeMoO}_6$ has shown that besides intergrain TMR, there exists a large intragrain magnetoresistance (MR), which appears near T_C , that is, around

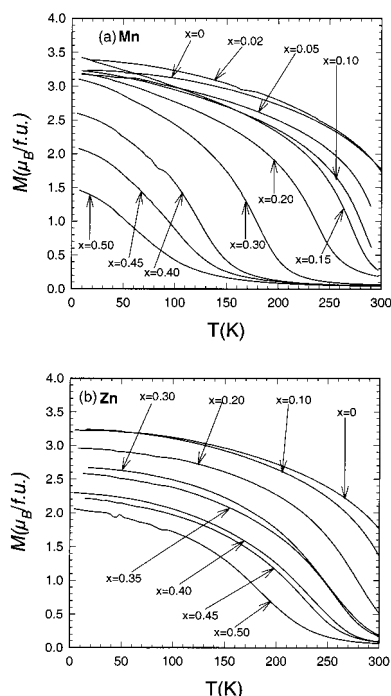


Figure 1. T -dependent magnetization (M) of the double-perovskites (a) $\text{Ba}_2\text{Fe}_{1-x}\text{Mn}_x\text{MoO}_6$ and (b) $\text{Ba}_2\text{Fe}_{1-x}\text{Zn}_x\text{MoO}_6$, registered in 1.45 T.

340 K.⁴ The role of the different species, Fe^{3+} and Mo^{5+} (or Re^{5+}), concerning the mechanism for the appearance of intergrain and intragrain negative MR, is to date not elucidated. In the present paper, we study the substitution of various divalent and trivalent elements for iron in $\text{Ba}_2\text{FeMoO}_6$. We show that the transport and magnetic properties around T_C of these oxides are significantly influenced by the substitution, T_C decreasing with the substitution level. Both intragrain MR and intergrain TMR at low temperature are observed,

* To whom correspondence should be addressed. Tel.: 33 2 31 45 26 37. Fax: 33 2 31 95 16 00. E-mail: christine.martin@ismra.fr.

(1) Kobayashi, K. I.; Kimura, T.; Sawada, H.; Terakura, K.; Tokura, Y. *Nature (London)* **1998**, *395*, 677.

(2) Hwang, H. Y.; Cheong, S. W.; Ong, N. P.; Batlogg, B. *Phys. Rev. Lett.* **1996**, *77*, 2041.

(3) Kobayashi, K. I.; Kimura, T.; Tomioka, Y.; Sawada, H.; Terakura, K.; Tokura, Y. *Phys. Rev. B* **1999**, *59*, 11159.

(4) Maignan, A.; Raveau, B.; Martin, C.; Hervieu, M. *J. Solid State Chem.* **1999**, *144*, 224.

(5) Kim, T. H.; Uehara, M.; Cheong, S. W.; Lee, S. *Appl. Phys. Lett.* **1999**, *74*, 1737.

(6) Garcia-Landa, B.; Ritter, C.; Ibarra, M. R.; Blasco, J.; Algarabel, P. A.; Mahendiran, R.; Garcia, J. *Solid State Commun.* **1999**, *110*, 435.

(7) Borges, R. P.; Thomas, R. M.; Cullinan, C.; Coey, J. M. D.; Suryanarayanan, R.; Ben-Dor, L.; Pinsard-Gaudart, L.; Revcolevski, A. *J. Phys. Condens. Matter.* **1999**, *11*, L 445.

(8) Prellier, W.; Snolyaninova, V.; Amlan Biswas, C.; Galley, R.; Greene, L.; Ramesha, K.; Gopalakrishnan, J. *J. Phys. Condens. Matter.* **2000**, *12*, 1.

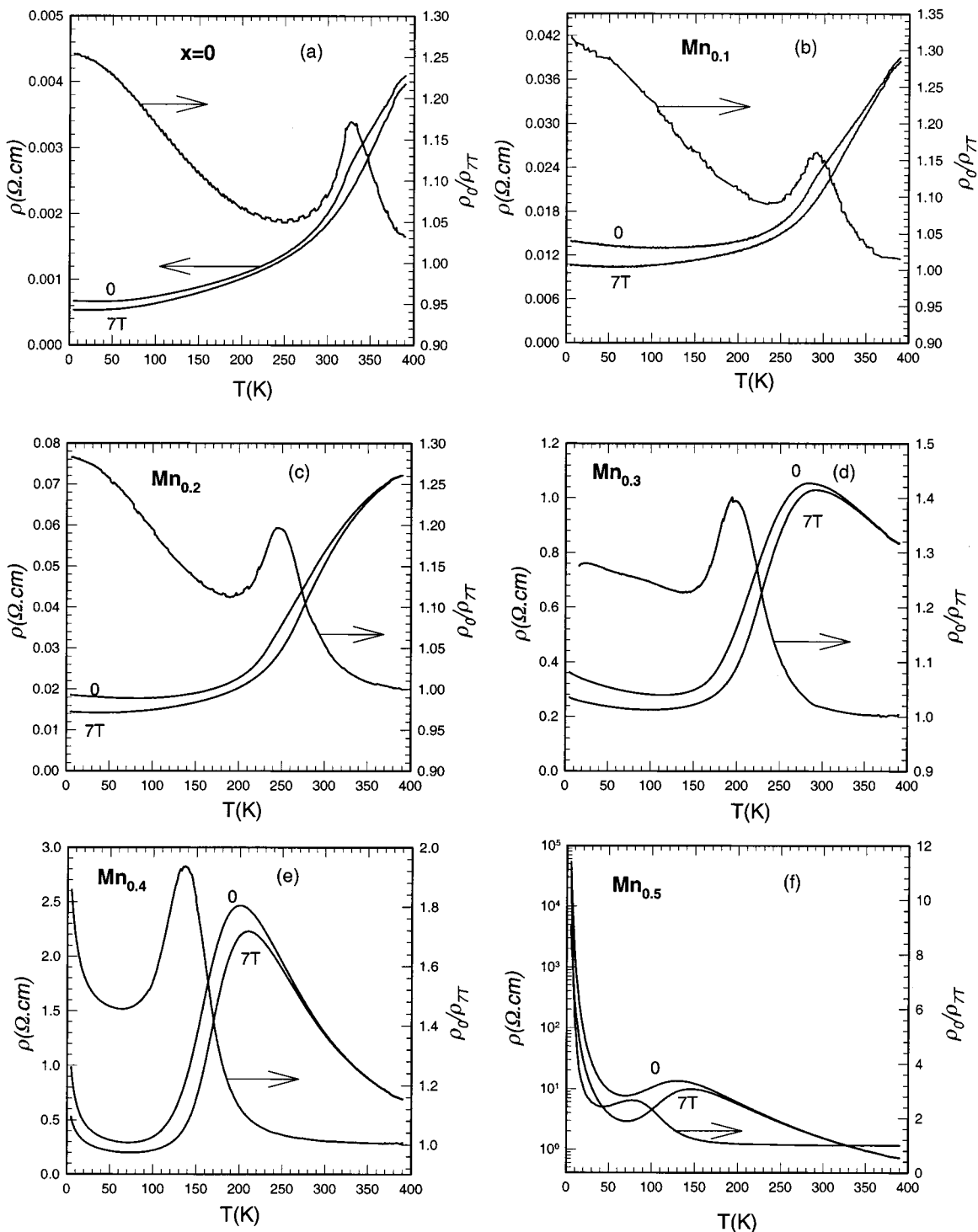


Figure 2. T -dependent resistivity (ρ) in $\text{Ba}_2\text{Fe}_{1-x}\text{Mn}_x\text{MoO}_6$ registered upon cooling in the absence of magnetic field and in 7 T; the T -dependent ρ_0/ρ_{7T} ratio is also shown (right y -axis). (a) $\text{Ba}_2\text{FeMoO}_6$,⁴ (b) $\text{Ba}_2\text{Fe}_{0.9}\text{Mn}_{0.1}\text{MoO}_6$, (c) $\text{Ba}_2\text{Fe}_{0.8}\text{Mn}_{0.2}\text{MoO}_6$, (d) $\text{Ba}_2\text{Fe}_{0.7}\text{Mn}_{0.3}\text{MoO}_6$, (e) $\text{Ba}_2\text{Fe}_{0.6}\text{Mn}_{0.4}\text{MoO}_6$, and (f) $\text{Ba}_2\text{Fe}_{0.5}\text{Mn}_{0.5}\text{MoO}_6$.

whatever the nature of the cations and whatever the substitution level in the solubility range. More importantly, exceptionally high TMR magnitudes are observed for the zinc oxides $\text{Ba}_2\text{Fe}_{1-x}\text{Zn}_x\text{MoO}_6$ with $x \leq 0.50$.

Experimental Section

The polycrystalline $\text{Ba}_2\text{Fe}_{1-x}\text{M}_x\text{MoO}_6$ samples ($M = \text{Mn, In, Y, Cr, Ca, Mg, and Zn}$) were prepared by solid-state reaction at high temperature. Stoichiometric amounts of BaO_2 , Fe_2O_3 , M_2O_3 (MO or MO_2), MoO_3 , and Mo were mixed, pressed into

bars, and sintered in evacuated silica ampules at 1100 °C for 12 h. A mixture of MoO_3 and Mo was used to respect the O_6 nominal stoichiometry.

X-ray powder diffraction patterns were registered at room temperature with a Philips vertical diffractometer using $\text{Cu K}\alpha$ radiation. Diffraction data were collected by step scanning over an angular range of $10^\circ \leq 2\theta \leq 110^\circ$ in increments of 0.02° . The data were analyzed by the Rietveld method using the FULLPROF program.

The magnetic measurements, as a function of the temperature, were performed with a vibrating sample magnetometer. After zero field cooling, a magnetic field of 1.45 T was applied;

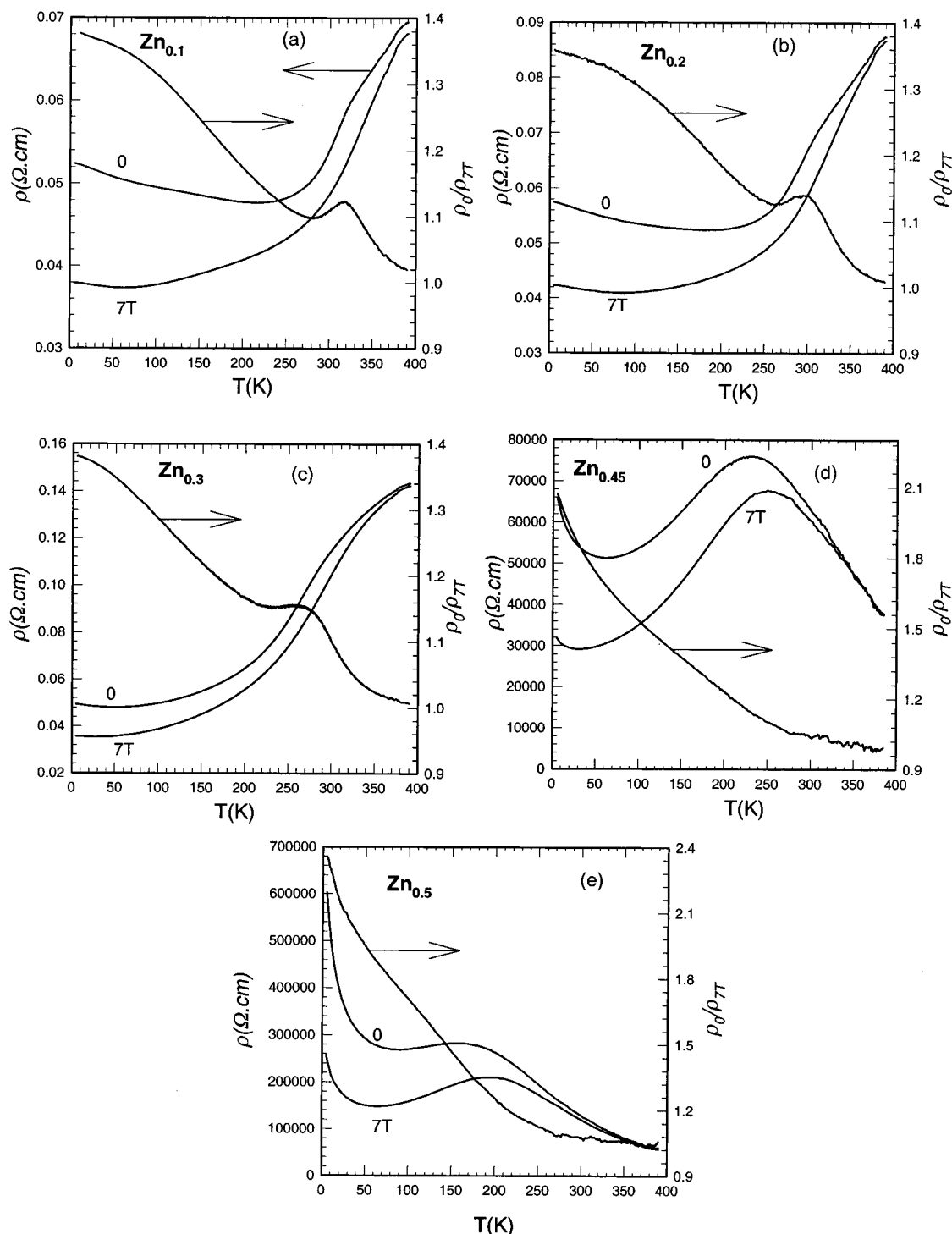


Figure 3. $\rho_0(T)$, $\rho_{7T}(T)$, and $\rho_0(T)/\rho_{7T}(T)$ curves for (a) $\text{Ba}_2\text{Fe}_{0.9}\text{Zn}_{0.1}\text{MoO}_6$, (b) $\text{Ba}_2\text{Fe}_{0.8}\text{Zn}_{0.2}\text{MoO}_6$, (c) $\text{Ba}_2\text{Fe}_{0.7}\text{Zn}_{0.3}\text{MoO}_6$, (d) $\text{Ba}_2\text{Fe}_{0.55}\text{Zn}_{0.45}\text{MoO}_6$, and (e) $\text{Ba}_2\text{Fe}_{0.5}\text{Zn}_{0.5}\text{MoO}_6$.

the magnetization was measured by increasing the temperature.

The resistivity measurements at zero field ($\rho(T)$) and under a magnetic field ($\rho(H)$) were performed with the PPMS (physical properties measurements system) Quantum Design model 6000, using the four-probe technique, for which four indium contacts were ultrasonically deposited onto the surface of bars with $2 \times 2 \times 10 \text{ mm}^3$ typical dimensions.

Results and Discussion

The substitution of divalent or trivalent cations for Fe^{3+} in $\text{Ba}_2\text{FeMoO}_6$ systematically increases the resistivity of the ceramic and decreases the ferromag-

netism whatever the nature of the cation, Zn^{2+} , Mg^{2+} , Ca^{2+} , Mn^{3+} , In^{3+} , Cr^{3+} , or Y^{3+} . This is illustrated by the two series $\text{Ba}_2\text{Fe}_{1-x}\text{Mn}_x\text{MoO}_6$ and $\text{Ba}_2\text{Fe}_{1-x}\text{Zn}_x\text{MoO}_6$. The $M(T)$ curves of these two series (Figure 1) confirm their ferromagnetic behavior, but show that their magnetic moment at 5 K decreases significantly as x increases, from $3.3\mu_B$ per formula unit for $x = 0$ to $1.5\mu_B$ for $x = 0.50$ in the Mn series (Figure 1a) and to $2.1\mu_B$ for $x = 0.50$ in the Zn series (Figure 1b). The M decrease with x is in agreement with the calculated one, deduced from the theoretical moments of $1\mu_B$ per Mo^{5+} , $5\mu_B$ per Fe^{3+} (high spin), and $4\mu_B$ per Mn^{3+} . Note that

the value obtained for the undoped sample is slightly smaller than the expected one for the antiferromagnetic coupling of the Mo^{5+} and Fe^{3+} spins. This divergence between the experimental and calculated magnetization values has been attributed to mis-site (Fe/Mo) imperfections.⁹ Moreover, the Curie temperature (T_C), measured at the inflection of the $M(T)$ curve, decreases significantly as the substitution level increases, from 330 K for $x = 0$ to 72 K for $x = 0.50$ in the Mn series and to 188 K for $x = 0.50$ in the Zn one. By optimizing x , in each series, T_C could be fixed at room temperature for instance.

The $\rho(T)$ curves registered under 0 and 7 T for the Mn series (Figure 2) show that these oxides exhibit a semimetallic behavior below T_C similar to that of the pristine one ($x = 0$) up to $x = 0.20$ (compare Figure 2a–c) with a change of slope at T_C . But the value of the zero field resistivity at 5 K increases significantly with x , from $7 \times 10^{-4} \Omega\text{cm}$ for $x = 0$ to $1.4 \times 10^{-2} \Omega\text{cm}$ for $x = 0.10$. Then, for $x = 0.30$, by decreasing T , a transition from a semiconducting to a semimetallic state is observed at $T_m = 280$ K, which does not coincide with $T_C = 180$ K (Figure 2d). For the larger doping levels, $x = 0.40$ and 0.50 (Figure 2e,f), a reentrant transition is also observed below ≈ 70 K. Note that the zero field resistivity for the last sample ($x = 0.50$, Figure 2f) reaches $10^5 \Omega\text{cm}$ at 5 K. All the substituted samples show a significant magnetoresistance effect under 7 T, in a large temperature range. The most remarkable feature deals with the evolution of the resistivity ratio, $(RR) = \rho/\rho_{7T}$, versus T , which goes through a minimum and then exhibits a maximum at T_C , that is, ranging from $T_C = 330$ K for $x = 0$ to 72 K for $x = 0.50$. The Zn series is characterized by a rather similar evolution of the resistivity versus temperature and versus x (Figure 3). Nevertheless, the resistivity of the $\text{Ba}_2\text{Fe}_{1-x}\text{Zn}_x\text{MoO}_6$ oxides is significantly higher than that for the Mn compounds, a transition from semimetal to a semiconducting like behavior is already observed at low temperature for $x = 0.10$ (Figure 3a) with a resistivity of $5.2 \times 10^{-2} \Omega\text{cm}$ at 5 K (to be compared to $1.4 \times 10^{-2} \Omega\text{cm}$ for $x = 0.10$ Mn sample); the $x = 0.20$ – 0.30 samples show similar $\rho(T)$ curves (Figure 3b,c), whereas from $x = 0.35$ to $x = 0.50$ a spectacular increase of the resistivity by several orders of magnitude is observed (Figure 3d,e). Like for the pristine compound and for the Mn series, the Zn series shows magnetoresistance, with a bump of the resistivity ratio at T_C for $x < 0.45$. Note however that for the same substitution level, the T_C is higher for zinc than for manganese and that the magnetoresistance at T_C does not vary significantly whatever the cation (Mn or Zn) and the level of substitution (x). For both series, the resistivity value at 5 K versus the doping level is reported in Figure 4. In these two series, the low-temperature resistivity jumps by several orders of magnitude beyond a critical x_c content of the doping elements, with $x_c = 0.40$ for Mn and Zn. This would suggest a percolation mechanism for the transport properties as previously reported in ref 11. In this framework, the foreign elements break

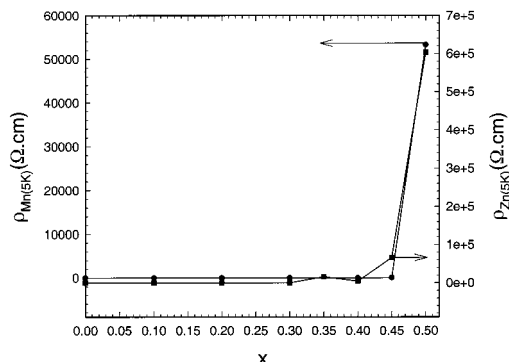


Figure 4. Resistivity at 5 K and 0 T versus doping level in the Mn (●) and Zn (■) series.

both the antiferromagnetic Fe–Mo coupling and thus the charge delocalization. Consequently, the size of the ferrimagnetic metallic regions will tend to decrease as x increases so that below the percolation threshold ($x > x_c$), the metallicity is suppressed. It should be pointed out that for x_c the low-temperature magnetization reaches $\approx 2.5 \mu_B/\text{f.u.}$ for Mn and Zn and thus this M value is similar to the value observed at x_c for $\text{Sr}_2\text{FeMo}_{1-x}\text{W}_x\text{O}_6$.¹¹ However, as pointed out in ref 11, the theoretical percolation threshold in the face-centered cubic (fcc) lattice is 0.195, which would correspond to $x_c \approx 0.8$ with the $\text{Ba}_2\text{Fe}_{1-x}\text{M}_x\text{MoO}_6$ formula. This value is much higher than the experimental one, $x_c \approx 0.4$. Thus, this suggests that the effect of the cationic substitution for Fe on the physical properties differs from the W for the Mo one. This could be explained by the larger cationic disordering on the B-site induced by Mn or Zn substitutions for Fe rather than W for Mo.⁹

A structural study has been performed for the Mn and Zn series. All the samples exhibit a $Fm\bar{3}m$ space group; the x dependence of the cell parameters is reported in Figure 5a for both systems. The increase of the a parameter with the substitution level is more important for Mn than for Zn, in agreement with the different cationic sizes.¹⁰ Note that impurities have been detected in a small amount, which decreases with x , and identified as BaMoO_4 and BaCO_3 (represented by \square and \circ respectively on the patterns in Figure 5b).

These results show without ambiguity that the MR peak observed above T_C corresponds mainly to bulk magnetoresistance; that is, the decrease of intragrain spin scattering due to the alignment of the local magnetic moments is improved either by magnetic field application or by temperature decrease below T_C . Substitutions carried out for several other species confirm this statement and show that this intragrain magnetoresistance, close to T_C , is systematically observed, whatever the nature of the substituting cation: Cr^{3+} , Mn^{3+} , In^{3+} , Y^{3+} , Zn^{2+} , Mg^{2+} , and Ca^{2+} . Thus, the temperature range for the appearance of MR will strongly depend on T_C . The evolution of T_C versus substitution level is shown in Figure 6 for different cations. It is remarkable that the size of the substituting cation serves to influence dramatically T_C . Considering the divalent cations, one indeed observes that for the same substitution level x , T_C decreases dramatically as the size of the cations increases: $T_C(\text{Zn}^{2+}) \sim T_C(\text{Mg}^{2+}) > T_C(\text{Ca}^{2+})$. A similar tendency is observed for trivalent cations. It is worth pointing out that the divalent cations

(9) Tomioka, Y.; Okuda, T.; Okimoto, Y.; Kumai, R.; Kobayashi, K. I.; Tokura, Y. *Phys. Rev. B* **2000**, *61*, 422.

(10) Shannon, R. D. *Acta Crystallogr.* **1976**, *A32*, 751.

(11) Kobayashi, K. I.; Okuda, T.; Tomioka, Y.; Kimura, T.; Tokura, Y. *J. Magn. Magn. Mater.* **2000**, *218*, 17.

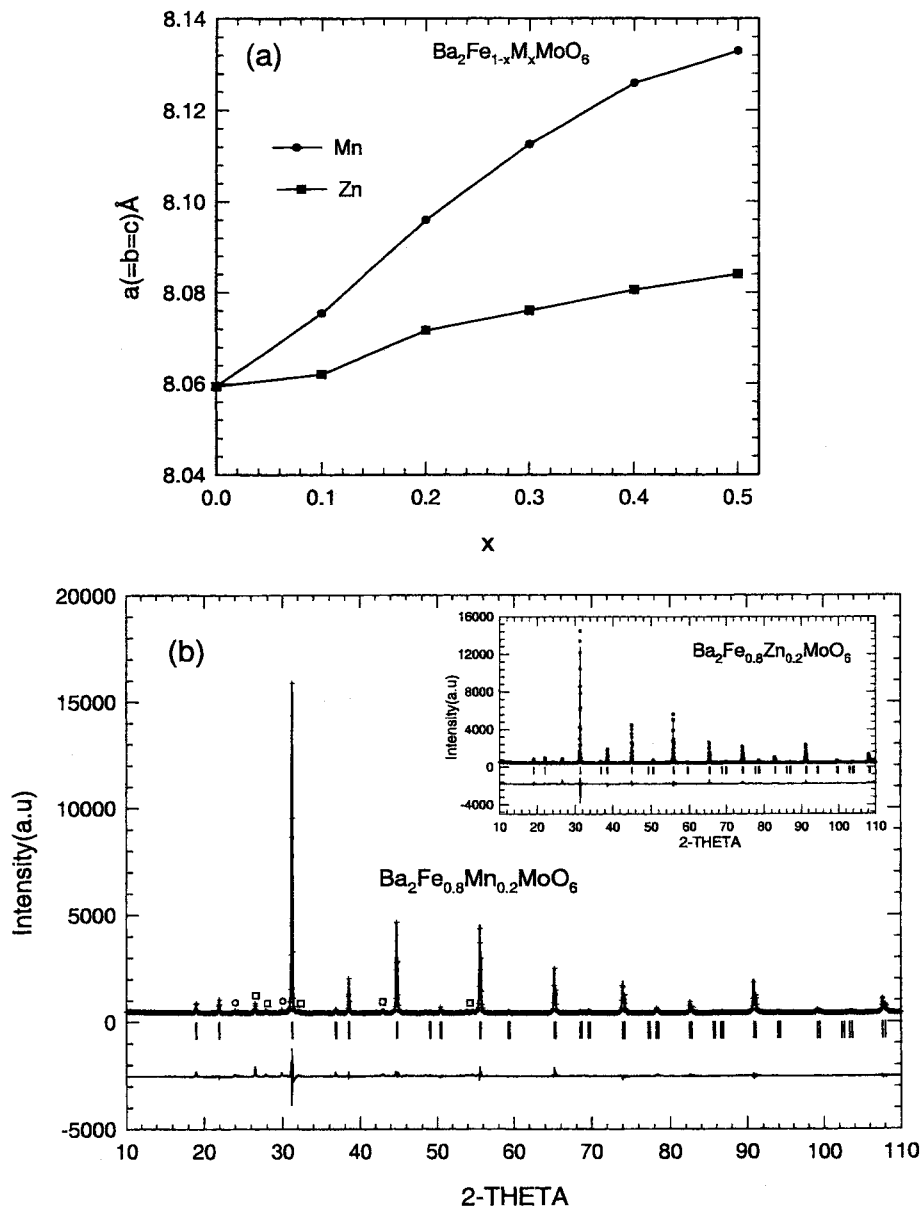


Figure 5. (a) Variation of the lattice parameters a with x for $\text{Ba}_2\text{Fe}_{1-x}\text{M}_x\text{MoO}_6$ ($M = \text{Mn, Zn}$) (b) The observed (.), calculated (—), and difference X-ray diffraction profiles of $\text{Ba}_2\text{Fe}_{0.8}\text{Mn}_{0.2}\text{MoO}_6$ and $\text{Ba}_2\text{Fe}_{0.8}\text{Zn}_{0.2}\text{MoO}_6$ in the inset. The squares and circles are for BaMoO_4 and BaCO_3 , respectively.

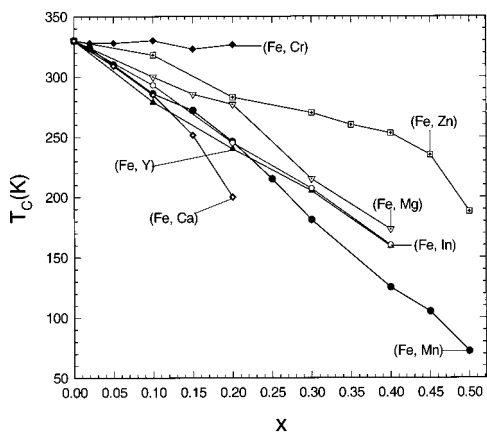


Figure 6. T_c versus substitution level (x) in $\text{Ba}_2\text{Fe}_{1-x}\text{M}_x\text{MoO}_6$.

M , such as Zn^{2+} and Mg^{2+} , induce the formation of Mo^{6+} , according to the equation $\text{Fe}^{3+} + \text{Mo}^{5+} \rightarrow \text{M}^{2+} + \text{Mo}^{6+}$. It is remarkable that the so-formed mixed-valent mo-

lybdenum $\text{Mo(V)}-\text{Mo(VI)}$ does not deteriorate significantly the intragrain transport properties of these materials.

To understand the influence of Fe-site substitutions upon the intergrain TMR properties of these oxides, resistivity measurements versus magnetic field were carried out at different temperatures. The $\rho(H)$ curves (Figure 7) show that a sharp decrease of the resistivity is obtained for low fields at 10 K, whatever the nature of the substituting cation, and even for a high substitution level. Under 0.2 T and at 10 K, the double perovskites $\text{Ba}_2\text{Fe}_{0.6}\text{M}_{0.4}\text{MoO}_6$ with $M = \text{Mn, In, Y,}$ and Mg exhibit rather similar MR values, where $\text{MR} = 100 \times [1 - \rho(H)/\rho(H=0)] \approx 4\%$ as shown for Mn in Figure 7a. In contrast, the zinc compound $\text{Ba}_2\text{Fe}_{0.6}\text{Zn}_{0.4}\text{MoO}_6$ exhibits an exceptionally high magnetoresistance (Figure 7b) of 22%, which could be related to its closeness to the critical concentration $x_c = 0.4$, separating the semimetallic from the semiconducting like compositions.

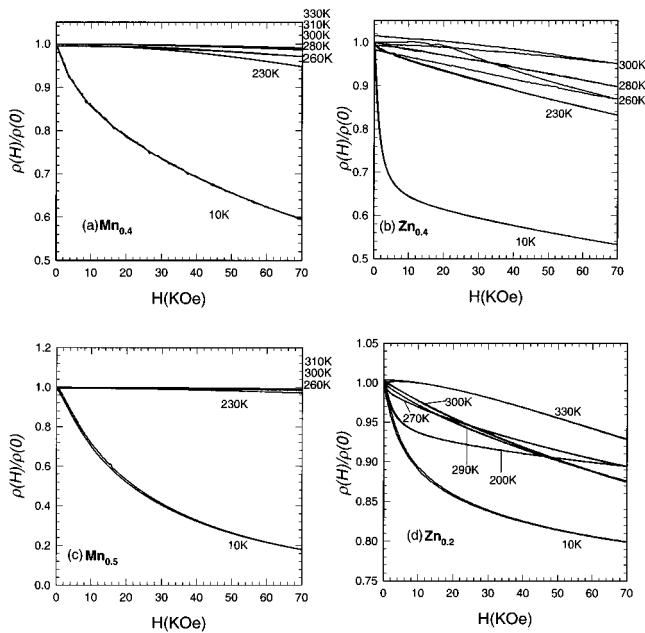


Figure 7. Isothermal magnetic field (H) dependence of the resistivity ratio $\rho(H)/\rho(0)$. T values are labeled on the graph, for (a) $\text{Ba}_2\text{Fe}_{0.6}\text{Mn}_{0.4}\text{MoO}_6$, (b) $\text{Ba}_2\text{Fe}_{0.6}\text{Zn}_{0.4}\text{MoO}_6$, (c) $\text{Ba}_2\text{Fe}_{0.5}\text{Mn}_{0.5}\text{MoO}_6$, and (d) $\text{Ba}_2\text{Fe}_{0.8}\text{Zn}_{0.2}\text{MoO}_6$.

The MR magnitude at the same temperature of 10 K but under 7 T for these compounds reaches very high values, such as 40% for Mn (Figure 7a) and 47% for Zn (Figure 7b). These magnetoresistance magnitudes at 10 K, often close to those previously observed for $\text{Sr}_2\text{FeMoO}_6$ ³ and $\text{Ba}_2\text{FeMoO}_6$,⁸ and even in some cases (as for Zn) significantly higher in low fields, clearly show that a very large substitution level of various elements for iron in $\text{Ba}_2\text{FeMoO}_6$ does not deteriorate the intergranular TMR at low temperature and in several cases such as zinc enhances it dramatically. The maximal magnetoresistance has been observed for $\text{Ba}_2\text{Fe}_{0.5}\text{Mn}_{0.5}\text{MoO}_6$, as shown in Figure 7c, with 81% at 10 K and 7 T, composition that again is close to the percolation threshold if one refers to Figure 2e and 2f. As expected, the magnitude of the intergrain MR in those samples decreases as the temperature increases and disappears close to T_C (Figure 7). Thus, from the application viewpoint it is clear that any substitution on the Fe site tends to decrease T_C and consequently should not be favorable to the appearance of intergrain TMR at room

temperature. Nevertheless, the TMR effect in the zinc compounds remains remarkable compared to $\text{Ba}_2\text{FeMoO}_6$ and even to $\text{Sr}_2\text{FeMoO}_6$. This is illustrated by the $\rho(H)$ curves of $\text{Ba}_2\text{Fe}_{0.8}\text{Zn}_{0.2}\text{MoO}_6$ (Figure 7d), which show that the MR of this phase at 290 K under 7 T is remarkably large, 12%, that is, close to those of $\text{Ba}_2\text{FeMoO}_6$ and $\text{Sr}_2\text{FeMoO}_6$, which are 15% and 9%, respectively, despite the lower T_C of this phase (290 K) compared to that of $\text{Ba}_2\text{FeMoO}_6$ (330 K) and $\text{Sr}_2\text{FeMoO}_6$ (475 K).

Conclusion

We have shown that the substitution of various divalent and trivalent cations for iron in the double-perovskite $\text{Ba}_2\text{FeMoO}_6$ affects significantly the magnetic and transport properties of this oxide, increasing the resistivity and decreasing both T_C and magnetization at low temperature. Nevertheless, the substituted oxides exhibit intragrain magnetoresistance characterized by a maximum around T_C . More importantly, it is observed that this substitution does not hinder the intergrain tunneling magnetoresistance in these double-perovskite oxides because the TMR effect is obtained for substitution levels as high as 40% on the Fe sites, and an exceptionally high MR magnitude under low field is observed for the zinc substituted oxide, MR = 22% in 0.2 T at 10 K. This remarkable intergrain TMR effect, observed for the zinc oxides, suggests that the doping may influence dramatically the quality of the grain boundaries and consequently the TMR properties. The preliminary ceramic microstructure study shows that, in our synthesis conditions, the average grain size does not vary significantly with the substitution, the diameter remaining around 2 μm , and that the density of the samples only slightly increases with the substitution level from 2.06 g/cm^3 for the undoped sample to 2.08 and 2.12 g/cm^3 for $\text{Ba}_2\text{Fe}_{0.5}\text{Mn}_{0.5}\text{MoO}_6$ with $M = \text{Zn}$ and Mn, respectively. A systematic study of these TMR properties, varying the sintering conditions, is needed to understand the transport properties in those oxides, which are most probably closely related to percolative phenomena. The exceptionally high MR value of -81% in 7 T at 10 K for $\text{Ba}_2\text{Fe}_{0.5}\text{Mn}_{0.5}\text{MoO}_6$, which lies close to the metal-insulator transition, is strongly in favor of such a model.

CM000929I